Electrostatic Attraction between Two Charged Surfaces: A (*N,V,T*) Monte Carlo Simulation

R. J.-M. Pellenq,† J. M. Caillol,‡ and A. Delville*,†

CRMD, CNRS (UMR6619), 1b rue de la Férollerie, 45071 Orléans Cedex 02, France, and MAPMO, CNRS (UMR6628), Département de Mathématiques, Université d'Orléans, BP6759, 45067 Orléans Cedex 02, France

Received: April 14, 1997; In Final Form: August 1, 1997[⊗]

We have performed (*N,V,T*) Monte Carlo simulations in order to study the stability of two parallel charged surfaces (lamellae) neutralized by exchangeable counterions. By varying each parameter characterizing the interface, *i.e.*, the interlamellar separation, the surface charge density of the lamellae, the dielectric constant of the solvent, and the radius and charge of the counterions, we have determined the stability of a wide class of physical situations. The ion−ion, lamella−ion, and lamella−lamella interactions are described within the context of the "primitive model". We give evidence that, despite the intrinsic simplicity of the primitive model, the phase diagram of such a system exhibits complex patterns. We have determined 2D contour maps of the equation of state in order to localize attracto/repulsive domains and optimize adhesive properties of the interface. This study concerns a large variety of lamellar materials, including hydrated cement and clays, and pillared and organo clays. At low dielectric constant, we have also found evidence of an attractive regime for lamellae neutralized by monovalent counterions.

I. Introduction

The stability of charged colloids[1,2] [latex, mineral oxides (clays, silica, ...), synthetic (polyacrylate, latex, ...) or natural (DNA, polysaccharides, ...) polyelectrolytes[3]] is generally discussed on the basis of the Deryaguin−Landau−Verwey−Overbeek (DLVO)[4−5] theory, which includes short-ranged van der Waals attraction and long-ranged electrostatic repulsion between the colloidal particles. This effective repulsion results from the entropy of colloidal suspensions which is estimated on the basis of the overlap between the ionic diffuse layers surrounding each polyion.[1,6−7] In the context of the primitive model,[8] calculations[9−10] or simulations[11−12] have already shown a net attraction between moderately coupled interfaces (*i.e.*, at weak interlamellar separation) neutralized by divalent counterions. However, these so-called attractive correlation forces[9−12] are ignored in the Poisson−Boltzmann treatment of charged interfaces, although this approximation underlies the DLVO theory.

In this article, we show the existence of complex phase diagrams from which the stability of charged lamellar materials [clays, organo, and pillared clays,[13,14] cement, lamellar oxides (aluminates, V_2O_5, silicates, ...)] can be predicted. We also report evidence of a *net attraction* between lamellae neutralized by *monovalent* counterions. In this case, the condition of strong coupling, necessary to observe such a behavior, is obtained by reducing the dielectric constant of the solvent. This result should provide new guidelines for the understanding of the stability of mixed systems,[13] *i.e.*, mixtures such as charged minerals (clays) neutralized by amphiphillic counterions (quaternary ammonium) in the presence of intercalated organic matter (organic solvent molecules, adsorbed reactant, ...). For such systems, the dielectric constants of both the lamellae and the intercalates are similar. Therefore, van der Waals attraction is strongly reduced and cannot contribute significantly to the pressure. As shown by our Monte Carlo simulations, the net interlamellar attraction results then mainly from electrostatic interactions, due to ionic correlations.

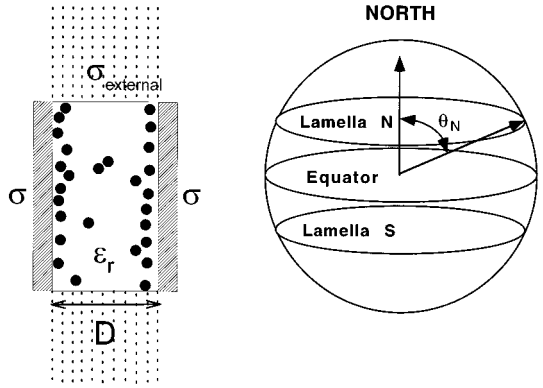

Figure 1. Scheme illustrating the calculation procedures in Euclidian (a, left) and hyperspherical (b, right) geometries.

We performed (*N,V,T*) Monte Carlo simulations[15] of the distribution of counterions neutralizing two infinite lamellae. We assume equality between the solvent and lamellar dielectric constant (no image charge).[16] The lamellae are structureless with uniform surface charge density, and no salt is added to the interface. In this case, the electrostatic interactions between parallel charged lamellae are optimal since the Debye screening length cannot be defined. The interactions between charged entities (counterions and lamellae) are described on the basis of the primitive model,[8] which includes contact hard core repulsion and long-ranged electrostatic interactions. Monte Carlo simulations are performed either within classical 3D Euclidian space[6,7,12,16−18] or on a hypersphere[19] (see Figure 1). The main advantage of this closed geometry[19−20] is to provide an exact analytical expression of Coulomb potential, without using long-range corrections or Ewald summations.[15] We have recently used Monte Carlo simulations on the hypersphere as a test of the approximate Euclidian approach, showing the equivalence of both procedures,[19] even for strongly coupled interfaces. Readers are referred to this article[19] which gives more details on the numerical procedures used for simulations within the hyperspherical geometry.

* Corresponding author.
† CRMD. E-mail: pellenq@cnrs-orleans.fr (for R. J.-M. Pellenq) and delville@cnrs-orleans.fr (for A. Delville).
‡ MAPMO. E-mail: caillol@labomath.univ-orleans.fr.
⊗ Abstract published in *Advance ACS Abstracts,* September 15, 1997.

S1089-5647(97)01273-X CCC: $14.00

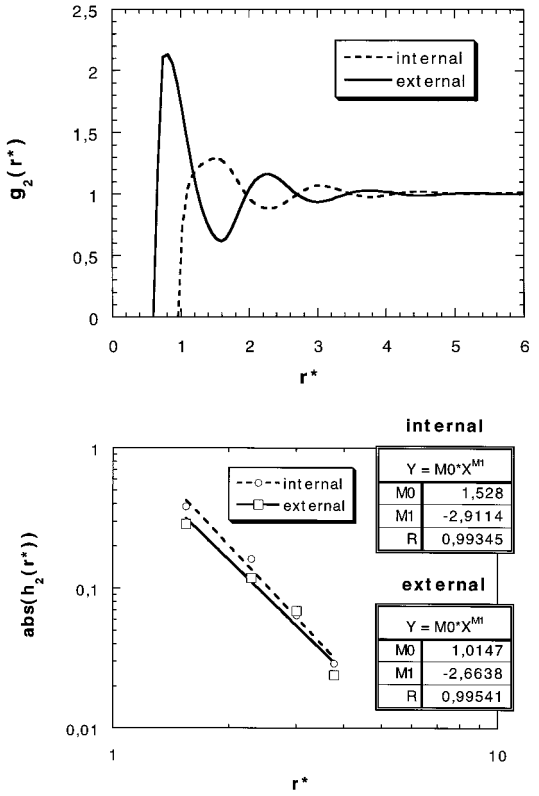

Figure 2. 2D radial distribution functions (a, top) of condensed counterions (see text) and radial decrease of their extrema (b, bottom).

We determine the equation of state of the charged interface from a calculation[21,22] of the longitudinal component of the pressure tensor. In the framework of the primitive model, the net longitudinal pressure of charged interfaces results from a balance between attractive electrostatic forces and repulsive contributions from ionic entropy and contact forces.[11−12,18−19] We use Monte Carlo simulations to generate equilibrium configurations of confined counterions and average the corresponding pressure of the interface. The same procedure was already used to determine the attractive regimes of charged lamellae neutralized by divalent counterions.[11,12,18,19]

By varying all parameters characterizing the ion/lamella coupling (*i.e.*, the interlamellar separation, the lamellar charge density, the ionic charge and radius, the dielectric constant of the solvent), we have analyzed the relative influence of energetic and entropic contributions to the swelling or cohesive behavior of charged interfaces. We have used 2D diagrams (pressure vs surface charge density and separation of the lamellae) to classify this diversity of mechanical properties and derive a criterion for optimum cohesion of charged interfaces. The strong attraction detected at low dielectric constant is also an intrinsic property of electrostatic interactions between charged interfaces. A careful description of these electrostatic interactions is thus required in order to understand the mechanical properties of charged interfaces (equation of state, swelling, phase separation,[23,24] order/disorder transitions,[25,26] aggregation,[25] flocculation, ...).

II. Methods

We use (*N,V,T*) Monte Carlo simulations[15] to determine the equation of state of colloidal suspensions of charged particles neutralized by mono-, di-, or polyvalent counterions. The electrical neutrality of the simulation cell is a necessary condition to reach the thermodynamic limit, in order to obtain results independent of the size of the simulation cell. The charged lamellae are structureless and infinite, with uniform surface charge density. In the context of the primitive model,[18] ions

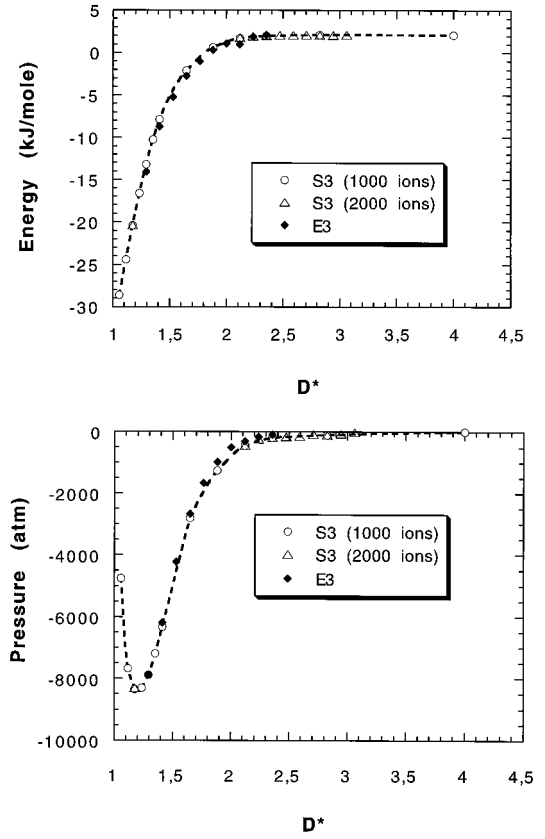

Figure 3. Comparison between swelling energy (a, top) and pressure (b, bottom) of charged interfaces calculated with Euclidian and hyperspherical geometries. The parameters characterizing the interface are the lamella charge density (σ = 0.02 electron/Å^2), the solvent dielectric constant (ϵ_r = 5), the ionic diameter (d_i = 4.25 Å), and the ionic valency (z_i = 1).

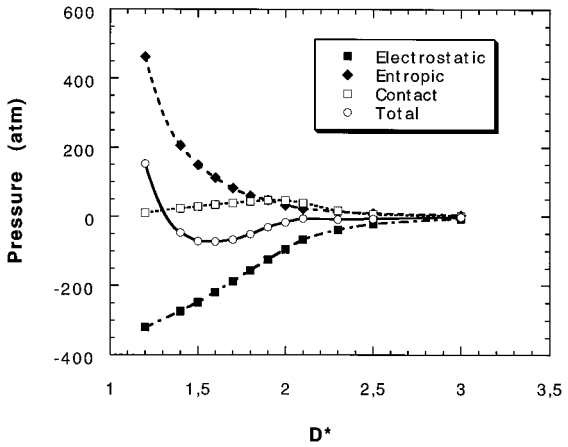

Figure 4. Total pressure and its different components (electrostatic, entropic, and contact) calculated for divalent ions (ionic diameter d_i = 6 Å) neutralizing lamellae with charge density 0.014 electron/Å^2 in presence of water.

interact through contact repulsion and long-ranged Coulomb potential. The solvent is described as a continuum, with uniform dielectric constant (ϵ_r), equal to the lamellar dielectric constant.

Two geometries are used for these simulations: Euclidian[6,7,11,12] and hyperspherical.[19] Within Euclidian geometry, the simulation cell is an asymmetrical slit pore (Figure 1a), limited in the longitudinal direction by two charged lamellae, while periodic boundary conditions are only applied in the lateral directions. Ion−ion, ion-lamella, and lamella−lamella interactions are calculated using 2D minimum image (MI) convention[15] along transverse directions. The MI procedure introduces a cutoff at the half-width of the simulation cell. In order to take into account the long-range character of Coulombic potential,

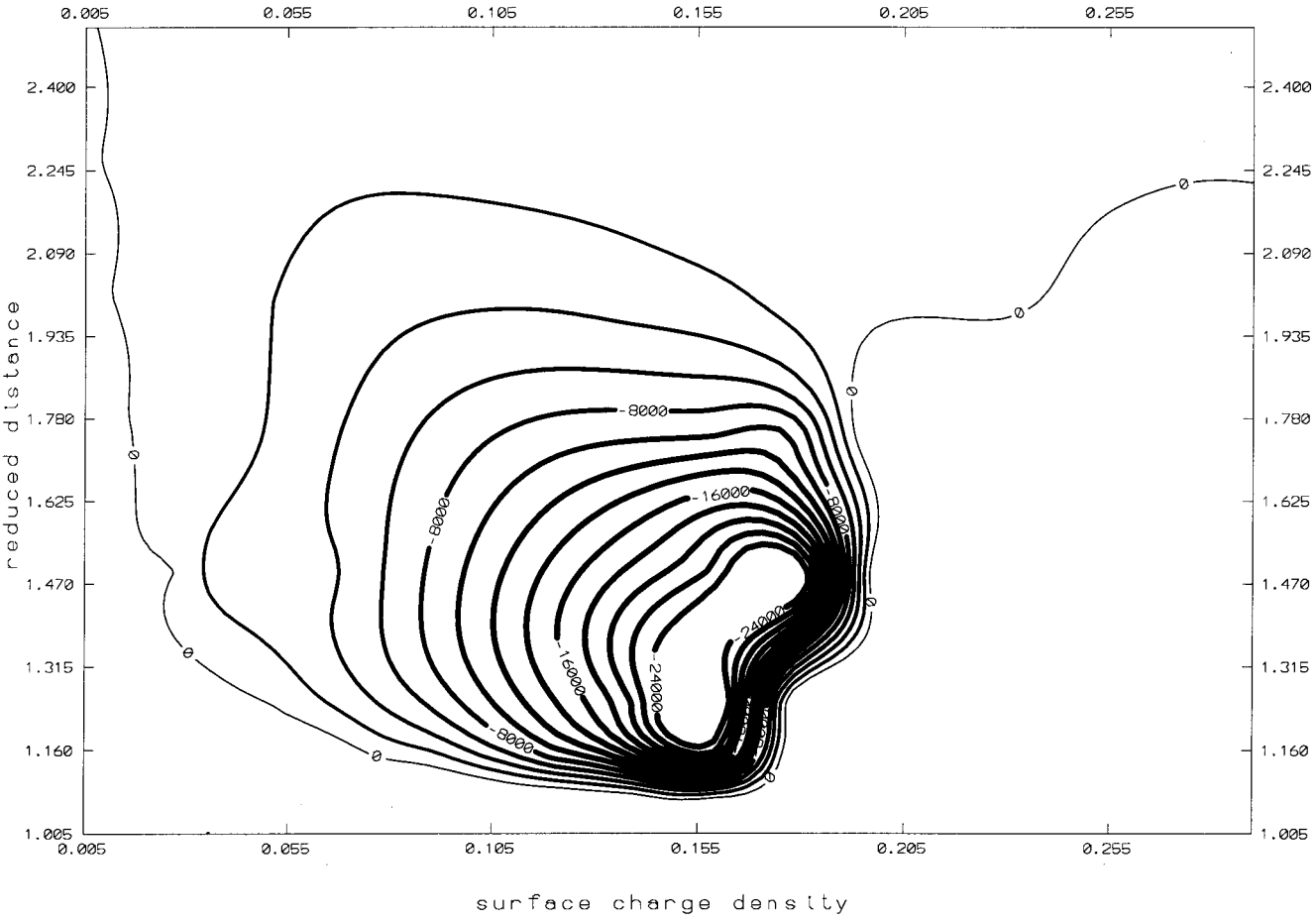
reduced distance
surface charge density
0.005
0.055
0.105
0.155
0.205
0.255
2.400
2.245
2.090
1.935
1.780
1.625
1.470
1.315
1.160
1.005
0
-8000
-16000
-24000

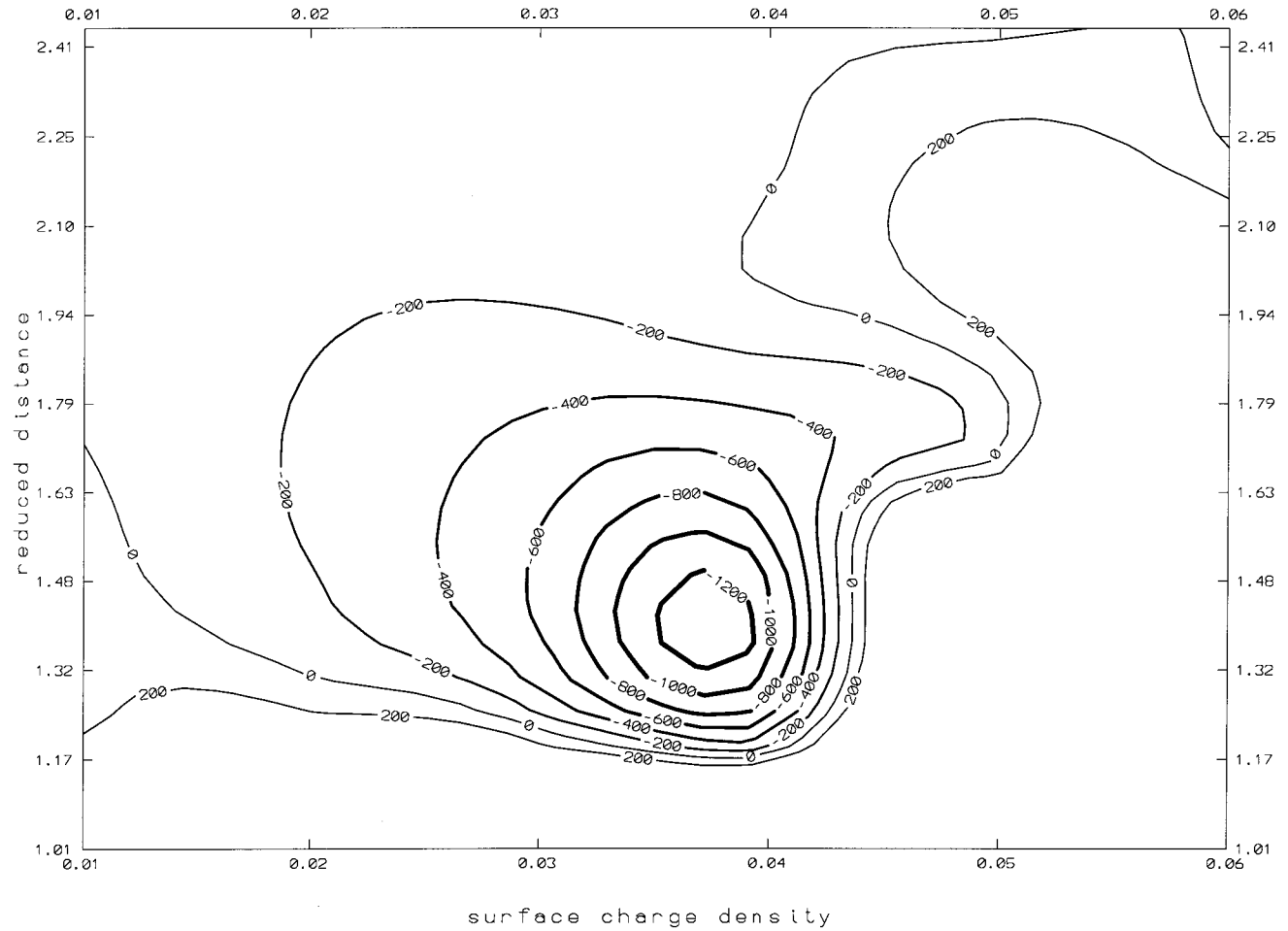
reduced distance
surface charge density
0.01
0.02
0.03
0.04
0.05
0.06
2.41
2.25
2.10
1.94
1.79
1.63
1.48
1.32
1.17
1.01
200
0
-200
-400
-600
-800
-1000
-1200

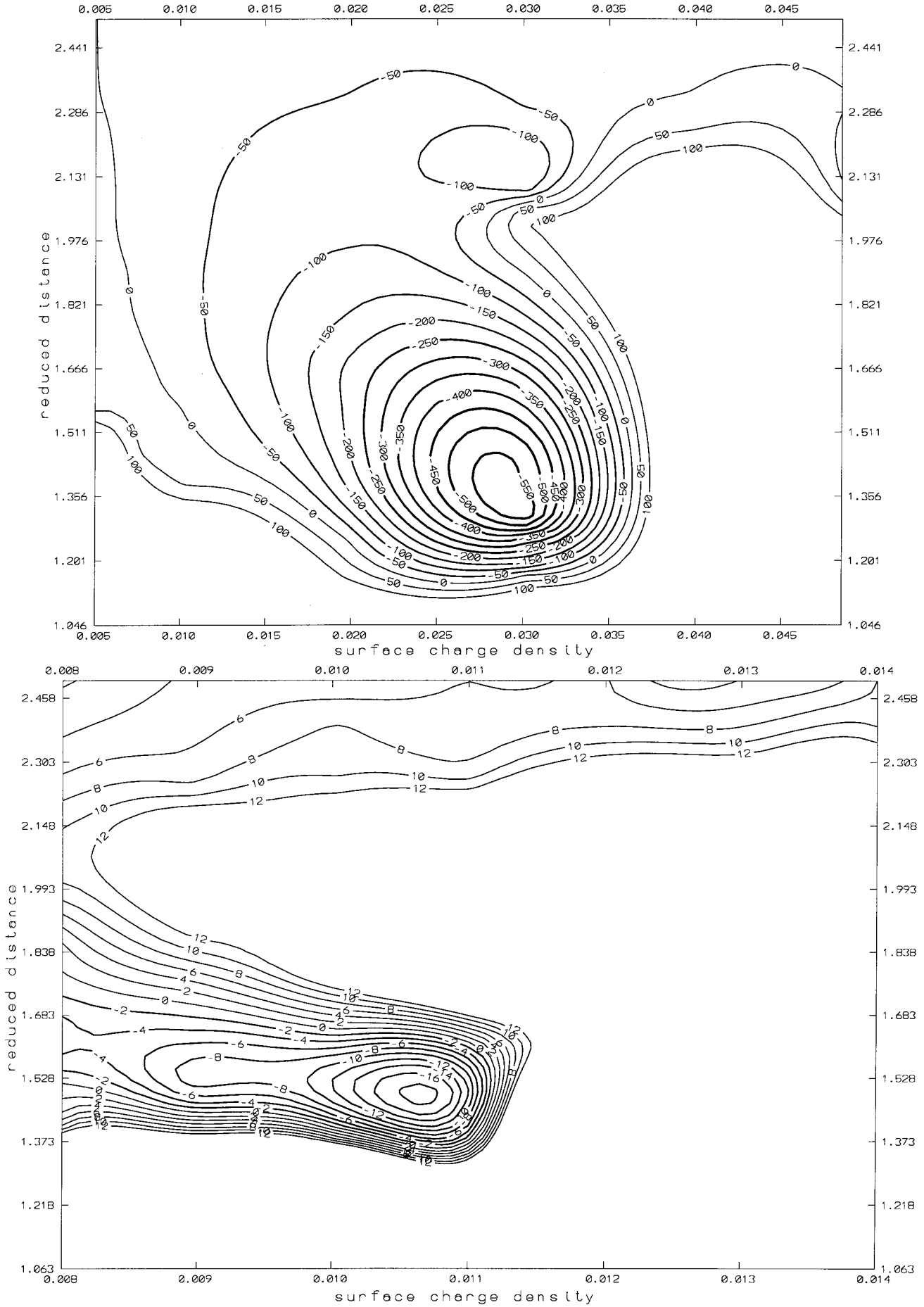

Figure 5. 2D contour plots of the swelling pressure in water of charged interface as a function of the interlamellar separation and the surface charge density. The neutralizing divalent counterions have ionic diameter respectively equal to (from top to bottom) 2 Å (a), 4.01 Å (b), 4.78 Å (c), and 8 Å (d).

an external potential is introduced following a self-consistent procedure (Figure 1a). This external Coulombic potential is generated by a set of virtual infinite planes parallel to the lamella surfaces, with a squared hole corresponding to the lateral section of the simulation cell. The surface charge density of the virtual planes is calculated in a self-consistent manner[6,7,16−18] from the longitudinal profile of condensed counterions (Figure 1a), using a standard block average procedure.[15] The charge density of the two planes surrounding the charged lamellae is obviously set equal to lamella charge density. This self-consistent procedure allows to introduce the long-range correction of Coulombic energy for a finite simulation box, by using a mean-field approximation. It should lead to reliable results if the lateral extend of the simulation cell exceeds the correlation length characterizing the counterion distribution.

As an example, Figure 2a displays 2D radial distribution functions of monovalent counterions (diameter 9 Å) confined between two charged lamellae (surface charge density of 5.5 $\times 10^{-2}$ electron/Å^2) at reduced separation $D^* = D/d_i = 1.78$ (where d_i is the ionic diameter). Figure 2a exhibits strong correlations between layers of ions at contact either with the same lamella (internal correlation) or with neighboring lamellae (external correlation). Furthermore, both radial structures do not decrease according to an exponential law, but much more slowly, according to an algebraic law [$\sim r^{(-3\pm0.3)}$] in agreement with theoretical predictions[27] (Figure 2b). As a consequence, no correlation length may characterize the lateral extent of the organization of confined counterions, *a priori* limiting the validity of the previous numerical procedure.

By contrast with the Euclidian geometry, the hypersphere (Figure 1b) is a closed system: ions and charged lamellae are localized at the surface of a sphere in a 4D Euclidian space. The simulation cell is also limited in the longitudinal direction by two parallel lamellae, but no periodic boundary conditions are needed since the space is closed. Numerical simulations of charged systems are easier to perform on a hypersphere[19] because simple analytical and exact expressions of Coulomb forces and potentials are available, without any Ewald summations or external potential to describe the long-range character of Coulombic interactions. This procedure is thus used to check the validity of the first approach.

After thermalization of the counterion distribution, block average[15] is used to calculate equilibrium properties of the charged interface (ionic concentration profile, energy, and pressure). Because of its anisotropy, longitudinal (normal to lamellae surface) and transverse components of the tensor pressure are different.[22] The virial theorem[21] is used to determine the swelling pressure of the interface from an expression of the local[22] longitudinal component of the pressure tensor. For that purpose, a fictitious surface, parallel to the charged lamellae, divides the simulation cell in two subvolumes. The longitudinal pressure is derived from the longitudinal component of the forces exerted between any pair of elements (ions or lamellae) located within different subvolume. An entropic contribution to the pressure is derived from the average local density of labile counterions (van't Hoff law). This last term is isotropic and positive, leading to a repulsive contribution to the longitudinal pressure. Note that the total pressure calculated in the (N,V,T) ensemble can be either positive or negative. In many experimental systems, the state variable is not extensive (V) but intensive (P). As a consequence, a system under attracto−repulsive interactions respectively collapses (negative pressure) or swells (positive pressure) spontaneously, in order to maintain its mechanical equilibrium.

The fictitious surface may be located anywhere in the interfacial domain, since, at equilibrium, the longitudinal pressure is constant within the interface (condition of mechanical equilibrium). In the context of Poisson−Boltzmann approximation (which neglects ionic correlation), the fictitious plane is located at the center of the interface and the entropic term is the only contribution to the swelling pressure. For symmetry reasons, the *average* electric field is zero at half interlamellar distance. However, *instantaneous* configurations of the confined counterions may deviate from this average, leading to oppositely charged subvolumes. A net instantaneous attraction thus appears for strongly coupled interfaces at weak interlamellar separations due to interionic correlations. This effect is similar to the electronic correlation also leading to a net attraction between molecules (the so-called London-dispersion interaction).

For pressure calculations on the hypersphere,[19] we have used a fictitious surface quenched between one charged lamella and the neutralizing counterions. The entropic contribution cancels out and the longitudinal pressure results from a balance between the ion−lamella contact repulsion ($P_z^{cont} = c_i\,(d_i)kT$, where d_i is the ionic diameter and $c_i\,(d_i)$ is the density of ions at contact with the lamella) and the electrostatic attraction between the isolated lamella and the other charges of the simulation cell:[19]

$$P_z = P_z^{cont} - \frac{\sigma^2}{2\epsilon_0\epsilon_r} \tag{1}$$

where σ is the charge density of the lamellae. The pressure is then simpler to derive since ion/lamella contact repulsion is the only unknown contribution. However, at high surface charge density, numerous counterions accumulate on the surface of charged lamellae and the absolute value of both terms in eq 1 increases, leading to large errors in their difference.[11] Nevertheless, numerical simulations on dense systems are more easy to perform on hypersphere,[19] because of its efficiency in handling hard core repulsions.[20] Thus, numerical simulations are performed using either Euclidian or hyperspherical geometry in order to take maximum advantages from their specific efficiency. We refer the reader to recent publications for more details on the calculation procedures using either the hyperspherical[19] or the Euclidian[11,12,18] geometry. As shown previously,[19] both approaches provide equivalent results for charged interfaces immersed in water ($\epsilon_r = 78.5$). We did not detect significant deviation of the energy (Figure 3a) or the pressure (Figure 3b) of charged interfaces immersed in organic solvent ($\epsilon_r = 5$).

Monte Carlo simulations are performed with 1000 counterions on hypersphere and 400 counterions in a 3D Euclidian cell. In both cases, at least 1 million iterations are performed for both thermalization and average steps of the Monte Carlo process.[15] The block size used for statistical average is at least equal to 28 000 iterations.

III. Results and Discussion

We derive the stability of charged interfaces from their equation of state (see section II). The pressure calculated from Virial theorem[21] is the sum of two components: entropic repulsion from labile counterions and energic contribution (Figure 4). In the context of the primitive model,[8] the second term includes again two components, resulting from hard core contact repulsions and electrostatic interactions. Finally, the electrostatic energy may be decomposed in three attracto−repulsive contributions: the ion−lamella attractions on the one hand and the ion−ion and lamella−lamella repulsions on the other hand. In all cases considered in this work, the net electrostatic contribution to the pressure is always attractive, but the balance between electrostatic, entropic, and hard-core contributions varies from attraction to repulsion as a function of the parameters characterizing the charged interface (interlamellar separation, ionic radius, and valency, lamella surface

charge density, dielectric constant of the constant of the solvent, ...). While each contribution is easily renormalized, the final balance cannot be predicted *a priori* from simple rules. We have thus performed systematic series of Monte Carlo simulations and derived contour maps of the equation of state in order to localize stability area of charged interfaces. This approach is applied to different classes of strongly coupled interfaces for which the equation of state is not monotonic, leading to complex phase diagrams and multiple phase coexistence.

Three classes of systems were considered in this study, differing by the nature of the solvent (characterized by its dielectric constant) and the neutralizing counterions (characterized by their radius and valency). First, we have considered divalent counterions (like Ca^{2+} and Mg^{2+}) and charged lamellae (clays, cement, ...) immersed in water; second, large monovalent counterions (quaternary ammonium) and charged lamellae (organoclays) immersed in organic solvent; and finally, large polyvalent counterions (aluminum oxides polymers) and charged lamellae (pillared clays) in presence of water.

The stability of charged interfaces was the subject of numerous Monte Carlo[6,7,10−12,16,17,28] or HNC[9−10,29] studies. However, large discrepancies were reported for results derived with point counterions,[6,11,28] since the neglect of hard-core ion−ion repulsion leads to excessive accumulation of counterions at the surface of the charged solids. The simplified model of point charges just describes the limiting behavior of the primitive model, with no experimental counterpart.

(A) Divalent Counterions in Water. Numerous studies using either Monte Carlo simulations[6,7,11,12,16−19] or numerical solutions[9,10,28] of integral equations were already devoted to these interfaces in order to explain the lack of swelling of Ca^{2+}-montmorillonite[30] whose surface charge density varies between 5×10^{-3} and 1.5×10^{-2} electron/Å^2.[31] Our study covers a broader range of charge densities (between 5×10^{-3} and 6×10^{-2} electron/Å^2). Note that 3×10^{-2} electron/Å^2 corresponds to the charge density of hydrated calciosilicates[32,33] which are responsible for the hardening of hydrated cement pastes. The numerical simulations are performed at four ionic radii (1, 2.05, 2.39, and 4 Å). The two intermediate cases correspond respectively to hydrated magnesium and calcium counterions.

Figure 5 displays the total pressure of these charged interfaces dispersed in water ($\epsilon_r = 78.5$); the entropic, hard-core, and electrostatic components of the pressure are further displayed in Figure 4. Despite the simplicity of the primitive model, Figure 5 exhibits a great variety of behaviors.

The first general feature of these charged interfaces is the reduced contribution of entropic repulsion (Figure 5). The major fractions of divalent counterions are located near to the lamellae because of the strong electrostatic coupling. Entropic repulsion becomes the major component of the pressure only under limiting conditions, *e.g.* reduced surface charge density or small interlamellar separation.

Another property is the deep attractive well occurring at interlamellar separations $1 < D^* < 4$ (D^* is the interlamellar separation divided by the ionic diameter), resulting again from strong electrostatic coupling (Figure 5). Finally, the contact pressure increases strongly with the surface charge density of the lamella. It reaches a maximum at separation $D^* \leq 2$ (Figure 4), which corresponds to the maximum overlap between the two parallel layers of condensed counterions. When the ionic radius increases from 1 to 4 Å, hard-core repulsion becomes large enough to cancel the electrostatic attraction or even to mask it totally (Figure 5). Another consequence of the nonmonotonic variation of hard-core repulsion is the coexistence

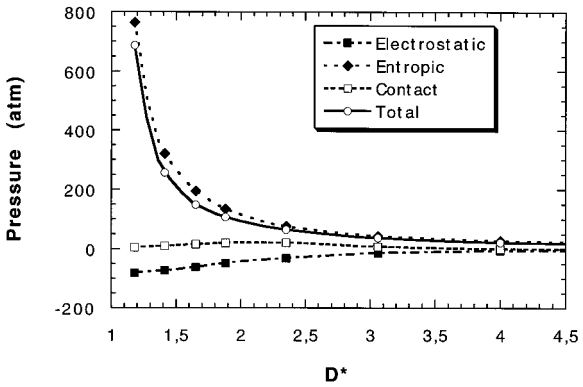

Figure 6. Total pressure and its different components (electrostatic, entropic, and contact) calculated for monovalent ions (ionic diameter 4.25 Å) neutralizing charge lamellae with charge density 0.007 electron/Å^2 in presence of water.

of two minima for a limited range of lamellar charge density (*e.g.* between 1.5×10^{-2} and 3.5×10^{-2} electron/Å^2 in Figure 5c).

Because of the strong attraction detected at charge density 0.03 electron/Å^2, we suggest that the electrostatic interactions between cement particles neutralized by calcium counterions could be at the origin of the setting of this class of lamellar materials.[32,33] By comparing 2D contour plots, we derive optimal conditions for interfacial cohesion of such systems. As an example, the decrease of the ionic radius shifts the pressure minimum toward larger surface charge densities. It also increases the deepness and the stiffness of the pressure well.

(B) Monovalent Counterions. Figure 6 displays the equation of state of Na^+ (ionic diameter 4.25 Å) montmorillonite (surface charge density 7×10^{-3} electron/Å^2)[29] dispersed in water. Both electrostatic attraction and hard-core repulsion are weaker than entropic repulsion. As a consequence, the equation of state is monotonic and the material swells perfectly in presence of bulk water, in agreement with experimental measurement.[30,31] Even in the presence of large exchangeable monovalent counterions, the primitive model predicts swelling of charged lamellae immersed in water. This relative weakness of energetic contributions allows to describe the swelling of this class of materials simply from ionic concentration profiles calculated from a solution of the Poisson−Boltzmann equation.[1,7] The neglect of ionic correlation is responsible for a limited (maximum 30%) overestimate of the swelling pressure.

Charged lamellar particles (like clays) may become organophilic if their neutralizing hydrophillic counterions (Li^+, Na^+, Ca^{2+}, ...) are exchanged by large hydrophobic ions (such as quaternary ammoniums[13]) which are generally tensioactive and organize themselves within micellar structures. These mixed systems exhibit complex phase equilibria which are far from totally understood, although numerous industrial applications (water treatment, heterogeneous catalysis, food, and cosmetic industries, ...) require a knowledge of their physicochemical properties (phase separation, flocculation, dispersion, ...).

Figure 7 displays the equation of state of charged lamellae neutralized by large monovalent counterions (ionic radius of 2.125, 3.16, 4.5, and 8 Å) dispersed in organic solvent ($\epsilon_r = 5$). The reduction of the dielectric constant enhances the electrostatic attraction responsible for the deep attractive well appearing at interlamellar separation smaller than $D^* \leq 2$ (Figure 7). As reported previously for divalent counterions in water (see section A), an increase of the lamellar surface charge density increases both electrostatic attraction and hard-core ion−ion repulsion. At large surface charge densities, hard core repulsion becomes the major component of the pressure, totally masking the electrostatic well (see Figure 7d).

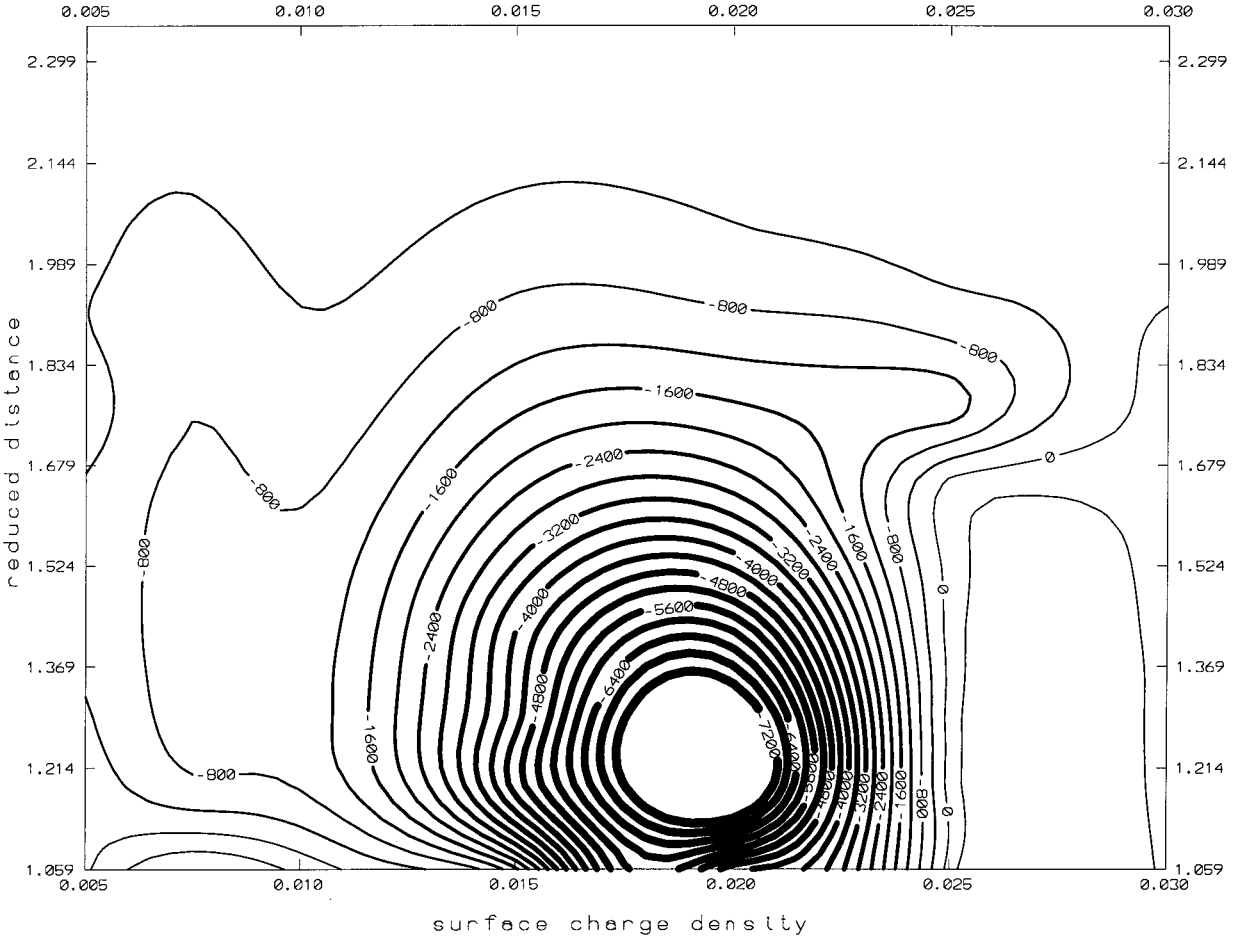
0.005
0.010
0.015
0.020
0.025
0.030
2.299
2.144
1.989
1.834
1.679
1.524
1.369
1.214
1.059
reduced distance
surface charge density
-800
-1600
-2400
-3200
-4000
-4800
-5600
-6400
-7200
0

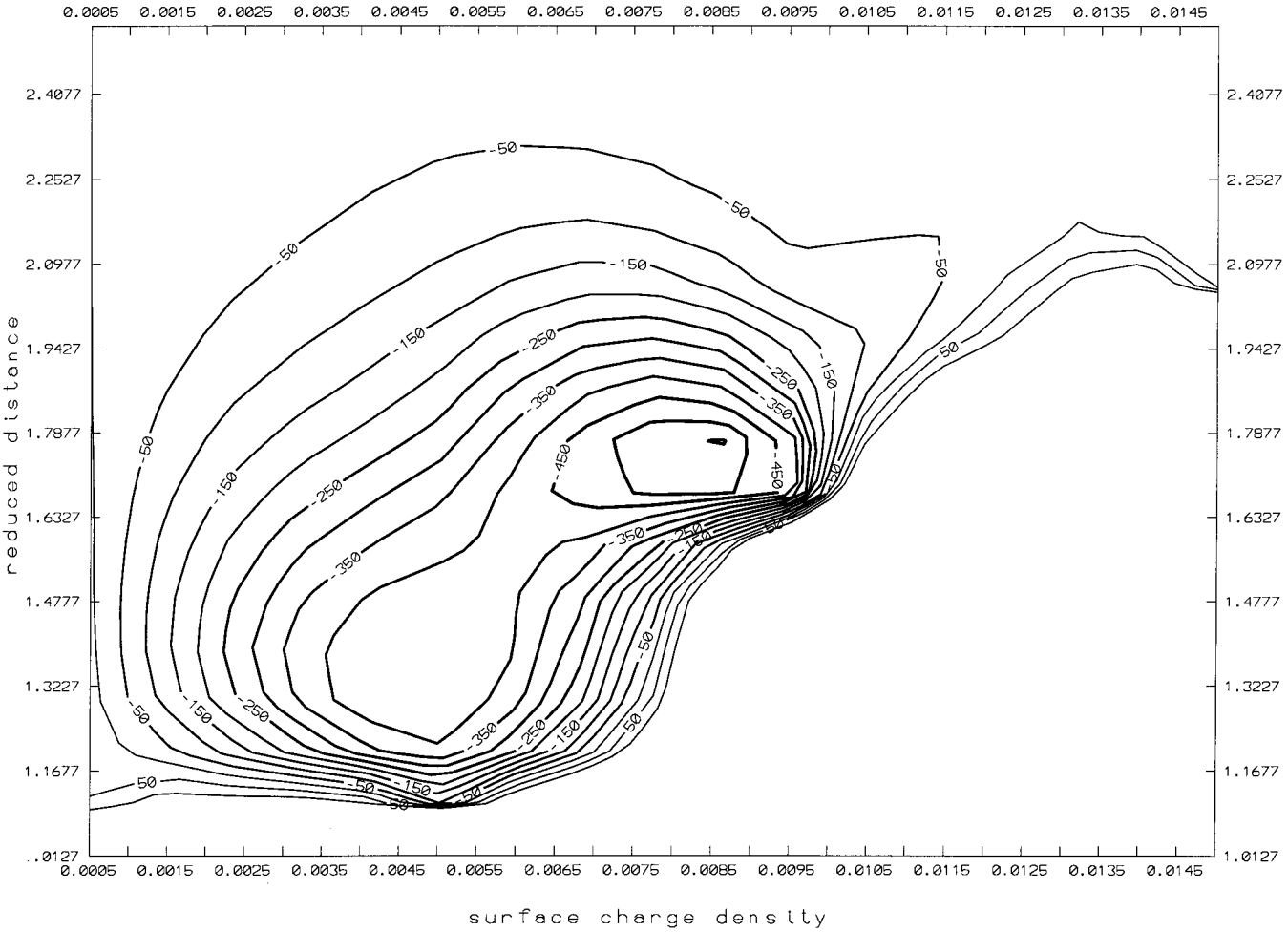
0.0005
0.0015
0.0025
0.0035
0.0045
0.0055
0.0065
0.0075
0.0085
0.0095
0.0105
0.0115
0.0125
0.0135
0.0145
2.4077
2.2527
2.0977
1.9427
1.7877
1.6327
1.4777
1.3227
1.1677
1.0127
reduced distance
surface charge density
-50
-150
-250
-350
-450

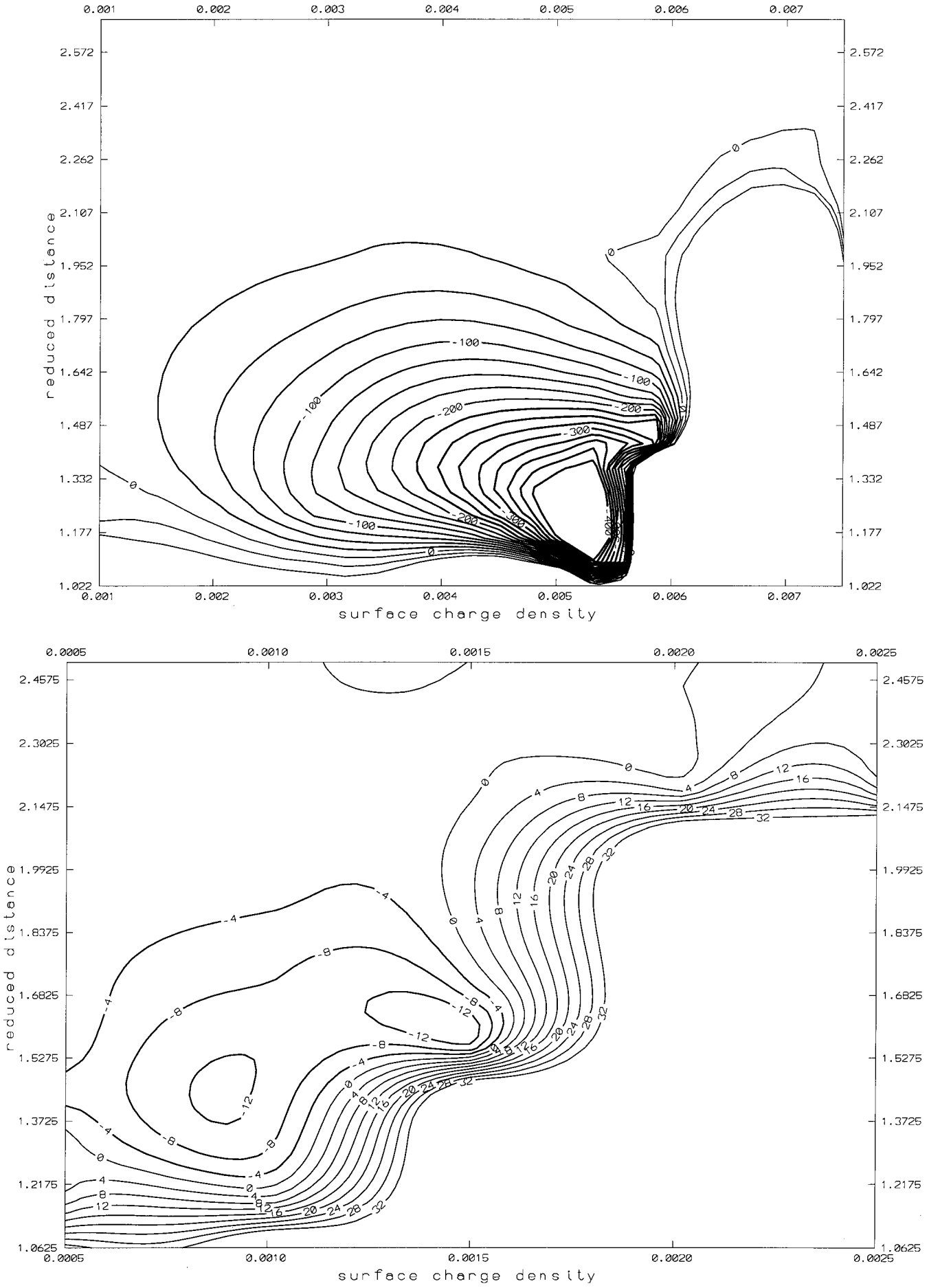

Figure 7. 2D contour plots of the swelling pressure in organic solvent ($\epsilon_r = 5$) of charged interface as a function of the interlamellar separation and the surface charge density. The neutralizing monovalent counterions have ionic radii respectively equal to (from top to bottom) 4.25 Å (a), 6.32 Å (b), 8.5 Å (c), and 16 Å (d).

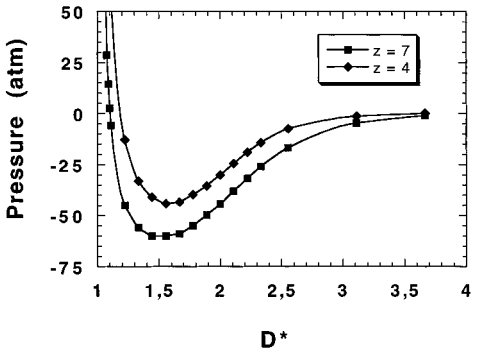

Figure 8. Swelling pressure in water of pillared clay (surface charge density 0.007 electron/Å^2) neutralized by tetra- and heptavalent counterions (ionic diameter 9 Å).

These results should be considered only as qualitative guidelines for the understanding and optimization of the behavior of mixed systems, since the primitive model neglects any specific interactions between ions, solvent molecules, and atoms forming the charged lamellae. However, classical DLVO theory, generally used to interpret biphasic systems, is unable to explain, in the present case, such phase coexistence. Indeed, strong van der Waals attraction is unlikely, because of the weak contrast between the solvent and lamellar dielectric constant.[1,2]

Polar solvent molecules, confined between two charged particles, organize themselves at the vicinity of the solid (for separation less than three molecular diameters) into layers parallel to the solid surfaces,[1,34] with preferential orientation of their dipole,[35] long residence time ($\approx 1\ \mu$s),[36] and large damping of their orientational fluctuations.[37] On the basis of the dynamical information deduced from NMR experiments[35−37] performed on water molecules in presence of clay particles, one may conclude that the dielectric constant of the phase of adsorbed water molecules should be smaller than that in the bulk. Therefore, swelling/cohesive behavior and phase coexistence of these highly confined interfaces can be dominated by net electrostatic attraction, even in the presence of monovalent counterions. Obviously, the oscillatory behavior of the pressure[38] detected in the same range of separations (as that measured with the surface force apparatus)[38] is due to hydration forces[1] and cannot be described without a molecular model of the solvent.[34,39]

(C) Polyvalent Counterions. Pillared clays are obtained from swelling clays by exchanging monovalent counterions by highly charged mineral counterions such as polymers of aluminum oxides (the so-called Al_{13} heptavalent counterion[13]). Although the high stability of these materials is not well understood, they are used as support for catalysts in important chemical processes (such as cracking, heterogeneous catalysis, ...) exploiting the selectivity offered by the porous network of the pillared mineral.

Figure 8 shows the equation of state of a pillared montmorillonite (ionic radius 4.5 Å and surface charge density of 7×10^{-3} electron/Å^2) in the presence of water ($\epsilon_r = 78.5$). Two types of counterions are considered (tetra- and heptavalent) since hydrolysis reduces the initial charge of intercalated aluminum oxide polymer. As expected from previous simulations on divalent counterions (see section A), high electrostatic attraction is responsible for the strong cohesion of the material. For surface charge density characterizing montmorillonite, ion−ion hard-core repulsion does not contribute significantly to the equation of state. The stability of such materials can thus be predicted on the basis of electrostatic interactions. From the results of section B, one expects further enhancement of the electrostatic attraction after replacement of water molecules by organic solvent.

(D) Universal Mapping of the Phase Diagram. From eq 1, we derive the general swelling condition of charged interfaces:

$$c_i(d_i/2)kT > \frac{\sigma^2}{2\epsilon_0\epsilon_r} \tag{2}$$

where c_i $(d_i/2)$ is the contact concentration of counterions. Defining F_{cond} as the ratio between contact and average ionic concentration (c_i°) and by using electroneutrality condition, one deduces the swelling criterion:

$$|\sigma| < \frac{eF_{cond}}{z_i\pi l_B(D - d_i)} \tag{3}$$

where d_i is the ionic diameter, z_i the ionic valency, $-e$ the electronic charge, D the interlamellar separation, and l_B the Bjerrum length [$l_B = e^2/(4\pi\epsilon_0\epsilon_r kT) = 7.143$ Å at room temperature in water]. The swelling condition then reduces to

$$F^*_{cond} = F_{cond}/F_{cond}^{ref} > 1 \tag{4}$$

by defining

$$F_{cond}^{ref} = \frac{|\sigma|ez_id_i(D^* - 1)}{4\epsilon_0\epsilon_r kT}$$

Figure 9 compares the fraction of contact counterions determined from Monte Carlo simulations and the analytical solution of the Poisson−Boltzmann (PB) equation.[40] Note that both PB and Monte Carlo procedures predict the same asymptotic linear variation of F_{cond} (Figure 9a) described by the definition of F_{cond}^{ref}. From our swelling condition (eq 4), we thus conclude that any positive or negative deviation of F_{cond} from its reference value leads respectively to net repulsion or attraction. At finite interlamellar distances ($D^* < 3$), the PB approximation predicts values of the fraction of contact counterions always larger than F_{cond}^{ref} (Figure 9a). In the same range of interlamellar distances, the fractions F_{cond} obtained by Monte Carlo simulations are generally smaller than F_{cond}^{ref} (Figure 9a). However, for high surface charge density ($|\sigma| \geq ez_i/2d_i^2$) and small interlamellar separations ($D^* < 2$), the fraction F_{cond} resulting from MC simulations becomes larger than the value estimated from the PB approach. In that case, excluded volume effects, neglected by the PB approximation, are responsible for strong interionic correlations (see Figure 2a). At such small distances, the Monte Carlo procedure may even be unable to generate highly compact monolayers of randomly distributed counterions.

Figure 9b clearly exhibits the influence of the interionic correlations on the stability of charged interfaces. The fraction $(F^*_{cond} - 1)$ renormalizes both electrostatic and contact interactions, simplifying the calculation of their balance:

$$P_z = \frac{\sigma^2}{2\epsilon_0\epsilon_r}(F^*_{cond} - 1) \tag{5}$$

The fraction $(F^*_{cond} - 1)$ includes the influence of both ionic condensation and interionic correlations on the longitudinal component of the pressure tensor. Although the treatment of PB equation always predicts a net repulsion between charged lamellae ($F^*_{cond} \geq 1$), Monte Carlo simulations may predict a net attraction ($F^*_{cond} < 1$) due to electrostatic interionic correlations, if the interlamellar volume is large enough ($ez_i/2|\sigma|d_i^2 > 1$). At higher lamellar charge density ($ez_i/2|\sigma|d_i^2 \leq 1$), the same Monte Carlo procedure predicts a net repulsion at small interlamellar separations ($1 < D^* < 2$), due to contact interactions. As a consequence, the mechanical behavior of

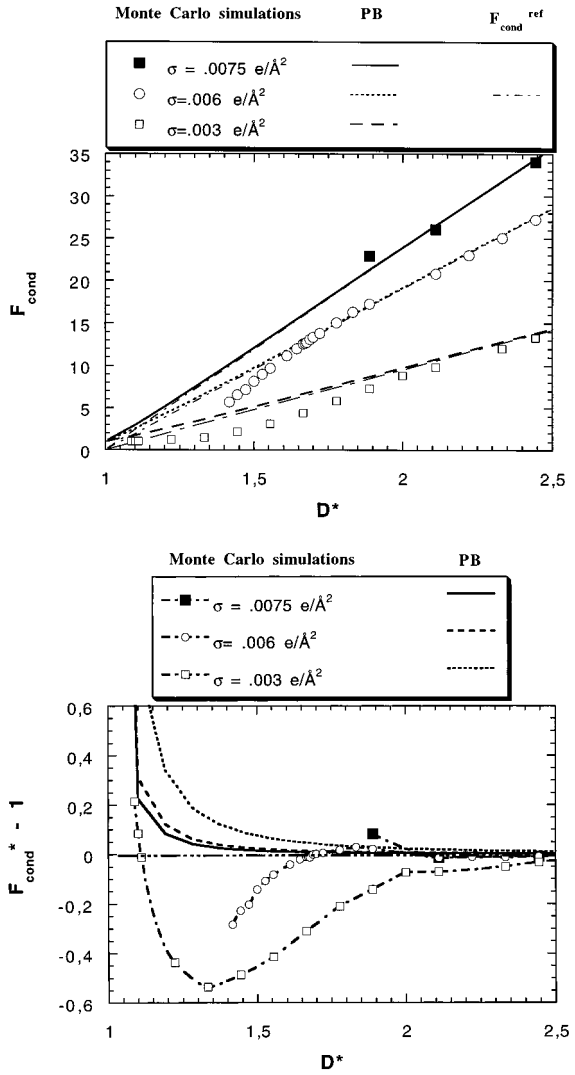

Figure 9. Comparison between the fraction of condensed ions F_{cond} (a, top) or its reduced form F^*_{cond} (b, bottom) predicted by Monte Carlo and Poisson−Boltzmann treatments (see text).

charged interfaces cannot be predicted *a priori* from simple analytical rules.

Nevertheless, our 2D plots highlight the coupling between the parameters characterizing the electrostatic and contact interactions, since these attracto−repulsive components of the pressure are both increasing functions of the surface charge density (in absolute values). By comparing the location of the deepest minima of Figures 5 and 7, we suggest criteria, valid in the range of parameters considered in this study, optimizing the adhesive property of charged interfaces:

$$D^* = 1.45 \tag{6a}$$

$$\sigma^*_{min} = 0.0177 \text{ (divalent ions in water)} \tag{6b}$$

$$= 0.07 \text{ (monovalent ions in organic solvent)}$$

where $\sigma^* = |\sigma|/|\sigma|^{ref}$, with $|\sigma|^{ref} = e\epsilon_r/z_i d_i^2$.

However, more studies are required in order to extrapolate our optimal stability condition to other systems, including those with an ionic valency larger than two. Finally, the possible secondary minimum of the pressure is located at the same optimal lamellar charge density, at interlamellar separation larger then 2, since contact pressure becomes than negligible.

From these results, we have drawn a universal contour map (see Figure 10), roughly localizing the pressure minima and the boundaries between attracto−repulsive area of the phase

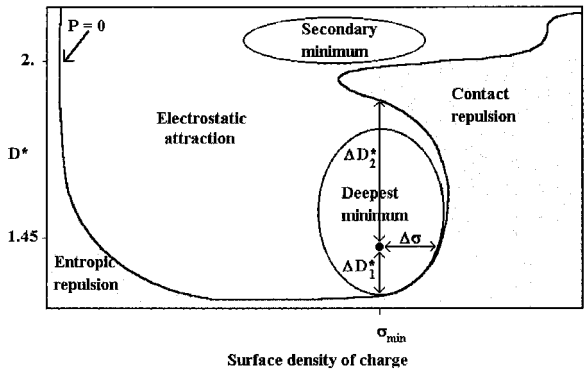

Figure 10. Universal contour map of the equation of state.

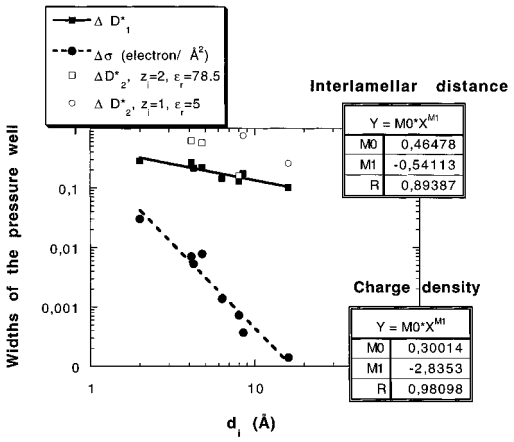

Figure 11. Widths of the pressure well (see section IIID) as a function of the ionic diameter.

diagram. Finally, we quantify the width of the attractive well from the distances between the pressure minimum and the neighboring repulsive domain. We define three parameters, $\Delta\sigma$, ΔD^*_1, and ΔD^*_2 (cf. Figure 10) characterizing the hardness of the material. The parameter ($\Delta\sigma$ and ΔD^*_1) varies as a power function of the ionic diameter (Figure 11) independently of the parameters characterizing electrostatic interactions. This result suggests that contact interaction is the major source of repulsion, as may be expected in that range of the phase diagram. Such general predictions should be very useful for optimizing the mechanical properties of charged lamellar materials. However, further simulations and theoretical treatments are required to understand the origin of such complex simplicity!

(E) Limitations and Overview. As already discussed,[19] the primitive model does not include a detailed description of all interactions between atoms composing these different classes of charged materials. However, no realistic model will be able to reproduce quantitatively the behavior of these highly coupled interfaces without a careful description of the long-ranged electrostatic interactions between their components. Our treatment based on the primitive model has to be considered as a first step in that direction.

Finally, this work concerns not only suspensions of mineral or synthetic colloids (clays, cement, silicate, latex, micelles, polyelectrolytes, ...) but also biopolymers[3] (proteins, DNA fragments, membranes, ...). For such colloidal systems, predictions based on numerical model of structureless infinite charged lamellae must be reconsidered, since shape[41] and size[24] effects may also modulate the extend of the diffuse layers and thus the strength of effective electrostatic coupling between the charged particles.

IV. Conclusions

We have performed (*N*,*V*,*T*) Monte Carlo simulations of the mechanical behavior of charged interfaces. From results

collected by a systematic variation of the parameters characterizing contact and electrostatic interactions, we have derived contour maps and localized attracto−repulsive regimes of a wide class of charged materials. These results explain the great variety of mechanical behavior of real systems, including clay swelling and cement setting. We also showed the influence of the nature of the counterion (characterized by its radius and valency) on the swelling of charged interfaces. Despite the simplicity of the primitive model, the predicted phase diagrams exhibit complex patterns. From the analysis of contour maps, we derive a universal contour map from which the boundaries of attracto−repulsive domains and the pressure minima may be localized. We have also detected the strong attractive regime and phase coexistence of dispersions in organic solvent of charged lamellae neutralized by monovalent counterions. These results clearly show that a careful description of electrostatic interactions of charged interfaces is required in order to quantitatively predict their mechanical properties.

Acknowledgment. Monte Carlo simulations were performed locally at the CRMD on HP 900−720 and 712 minicomputers and on Cray C98 supercomputer of IDRIS (CNRS, Orsay). We thank Dr. H. van Damme for helpful discussions.

References and Notes

(1) Israelachvili, J. N. *Intermolecular and Surface Forces*; Academic Press: London, 1985.
(2) Lyklema, J. *Fundamentals of Interface and Colloid Science*; Academic Press: London, 1991.
(3) Schmitz, K. S. *Macro-ion Characterization: From Dilute Solutions to Complex Fluids*; ACS Symp. Ser 548; American Chemical Society: Washington, 1994.
(4) Derjaguin, B.; Landau, L. D. *Acta Physicochim. URSS* **1941**, *14*, 635.
(5) Verwey, E. J. W.; Overbeek, J. T. G. *Theory of the Stability of Lyophobic Colloids*; Elsevier: New York, 1948.
(6) Jönsson, B.; Wennerström, H.; Halle, B. *J. Phys. Chem.* **1980**, *84*, 2179.
(7) Delville, A.; Laszlo, P. *New J. Chem.* **1989**, *13*, 481.
(8) Carley, D. D. *J. Chem. Phys.* **1967**, *46*, 3783.
(9) Kjellander, R.; Marcelja, S.; Pashley, R. M.; Quirk, J. P. *J. Phys. Chem.* **1988**, *92*, 6489.
(10) Kjellander, R.; Åkesson, T.; Jönsson, B.; Marcelja, S. *J. Chem. Phys.* **1992**, *97*, 1424.
(11) Guldbrand, L.; Jönsson, B.; Wennerström, H.; Linse, P. *J. Chem. Phys.* **1984**, *80*, 2221.
(12) Valleau, J. P.; Ivkov, R.; Torrie, G. M. *J. Chem. Phys.* **1991**, *95*, 520.
(13) Theng, B. K. G. *The Chemistry of Clay-Organic Reactions*; A. Hilger: London, 1974.
(14) Yamada, H.; Azuma, N.; Kevan, L. *J. Phys. Chem.* **1995**, *99*, 2110.
(15) Allen, M. P.; Tildesley, D. J. *Computer Simulation of Liquids*; Oxford Science Publishers: Oxford, U.K., 1994.
(16) Torrie, G. M.; Valleau, J. P.; Patey, G. N. *J. Chem. Phys.* **1982**, *76*, 4615.
(17) van Megen, W.; Snook, I. *J. Chem. Phys.* **1980**, *73*, 4656.
(18) Pellenq, R. J.-M.; Delville, A.; van Damme, H. *Characterization of Porous Solids IV*; Rouquerol, J., Rodriguez-Reinoso, F., Sing, K. S. W., Unger, K. K., McEnaney, B., Eds.; Elsevier: New York, in press.
(19) Delville, A.; Pellenq, R. J.-M.; Caillol, J. M. *J. Chem. Phys.* **1997**, *106*, 7275.
(20) Caillol, J. M.; Levesque, D. *J. Chem. Phys.* **1991**, *94*, 597.
(21) Hansen, J. P.; McDonald, I. R. *Theory of Simple Liquids*; Academic Press: London, 1986.
(22) Rao, M.; Berne, B. J. *Mol. Phys.* **1979**, *37*, 455.
(23) Lekkerkerker, H. N. W.; Poon, W. C.-K.; Pusey, P. N.; Strootbants, A.; Warren, P. B. *Europhys. Lett.* **1992**, *20*, 559.
(24) Mourchid, A.; Delville, A.; Lambard, J.; Lécolier, E.; Levitz, P. *Langmuir* **1995**, *11*, 1942.
(25) Langmuir, I. *J. Chem. Phys.* **1938**, *6*, 873.
(26) Onsager, L. *Ann. N.Y. Acad. Sci.* **1949**, *51*, 627.
(27) Jancovici, B. *Fundamentals of Inhomogeneous Fluids*; Henderson, D., Ed.; M. Dekker: New York, 1992; p 201.
(28) Wennerström, H.; Jönsson, B. *J. Phys. Fr.* **1988**, *49*, 1033.
(29) Greathouse, J. A.; McQuarrie, D. A. *J. Colloid Interface Sci.* **1996**, *181*, 319.
(30) Norrish, K. *Discuss. Faraday Soc.* **1954**, *18*, 120.
(31) Viani, B. E.; Low, P. F.; Roth, C. B. *J. Colloid Interface Sci.* **1983**, *96*, 229.
(32) Hamid, S. A. *Z. Kristallogr.* **1981**, *154*, 189.
(33) Viehland, D.; Li, J.-F.; Yuan, L.-J.; Xu, Z. *J. Am. Ceram. Soc.* **1996**, *79*, 1731.
(34) Delville, A. *J. Phys. Chem.* **1993**, *97*, 9703.
(35) Delville, A.; Grandjean, J.; Laszlo, P. *J. Phys. Chem.* **1991**, *95*, 1383.
(36) Delville, A.; Letellier, M. *Langmuir* **1995**, *11*, 1361.
(37) Petit, D.; Korb, J. P.; Delville, A.; Grandjean, J.; Laszlo, P. *J. Magn. Reson.* **1992**, *96*, 252.
(38) Israelachvili, J. N.; Pashley, R. M. *Nature* **1983**, *306*, 249.
(39) Boek, E. S.; Coveney, P. V.; Skipper, N. T. *Langmuir* **1995**, *11*, 4629.
(40) Engström, S.; Wennerström, H. *J. Phys. Chem.* **1978**, *82*, 2711.
(41) Chang, F.-R. Ch.; Sposito, G. *J. Colloid Interface Sci.* **1994**, *163*, 19.